Journal of Statistical Physics, Vol. 55, Nos. 5/6, 1989

Turbulence without Strange Attractor

U. Brosa[1]

Received January 15, 1988

It is shown that pipe-flow turbulence consists of transients. The "fractal" dimensions of the dynamical process are thus all zero. Nevertheless, this is compatible with Grassberger–Procaccia analyses suggesting the existence of a high-dimensional strange attractor. The usefulness of the Grassberger–Procaccia method to detect the aging of transients is demonstrated.

KEY WORDS: Chaos; fractal dimensions; intermittency; Navier–Stokes equation; pipe flow; strange attractor; turbulence.

1. INTRODUCTION

In a recent paper, Grassberger[1] complained about the slow acceptance of new notions on dynamical systems by practitioners. The various *fractal dimensions* which can be assigned to dynamical systems having *strange attractors* belong to these notions.[2] Now one semipractical application of fractal dimensions is connected with the need for a minimum description of a dynamical system: When its fractal dimension ν is, for example, 2.05..., then an autonomous system with at least three first-order differential equations is necessary to cope with the most important properties of the dynamics. To find the Grassberger–Procaccia fractal dimension ν requires only small effort.[3] Furthermore, it can be shown that all the other dimensions must be of similar size, so that the Grassberger–Procaccia dimension is representative and sufficient for the purpose just addressed. I will demonstrate here that the Grassberger–Procaccia method rather than the number ν itself gives useful information on a dynamical system even if it has no strange attractor.

Turbulence is thought to be the best example of a chaotic system. Fortunately, both terms, turbulence and chaos, are so elastic that this

[1] HLRZ c/o KFA Jülich GmbH, D-5170 Jülich, West Germany.

0022-4715/89/0600-1303$06.00/0

association cannot be wrong. In turbulence, one has to distinguish at least between two different kinds: turbulence with external body forces and turbulence dominated by shear flow. Examples for the first kind occur in the Raleigh–Bénard and Taylor systems. The body force in the Rayleigh–Bénard system is gravitation, which comes into play via thermal effects; in the Taylor system, the body force is centrifugal. These forces cause various instabilities, keep the fluid always in motion, and are thus prerequisites for this kind of turbulence. In shear-flow systems, as, e.g., in ordinary pipe flow, external body forces do not exist; turbulence must sustain imself merely by the friction between layers with different velocities and by inertia. The shear flows constitute thus a second kind of turbulent system.

Common to all them is the assignment of a *critical parameter*: For the Rayleigh–Bénard system, it is the *Rayleigh number*; for Taylor's system, it is the *Taylor number*; for the shear-flow systems, the *Reynolds number*. Turbulence arises when the critical parameter transgresses a certain value. But a closer inspection reveals important differences.

First, the onset is different. Turbulence in body-force systems is preceded by at least one linear instability.[4] For example, there is a critical Rayleigh number for the first instability Ra_1 and a Rayleigh number for turbulence Ra_{turb} with $Ra_1 < Ra_{\text{turb}}$. In the shear-flow systems we can have turbulence for Reynolds numbers which are much too small for an instability (channel flow is an example[5] with $Re_1 = 5772$ and $Re_{\text{turb}} \approx 1100$), or we can have turbulence when there is no linear instability at all (as in pipe flow[6] with $Re_{\text{turb}} \approx 2000$). Moreover, in all shear flows the critical Reynolds number Re_{turb} is not well defined, since it depends on the strength of the disturbances.

Second, the developed turbulence is different. For turbulence in body-force systems, Grassberger–Procaccia analyses indicated low-dimensional strange attractors.[3,7–10] For the shear flows, the same analysis yielded no finite dimension, and this holds true for analyses based on experimental and on computed data.[11,12] I will show here that the results for shear flow are compatible with turbulence which consists just of transients.

2. NO LOW-DIMENSIONAL STRANGE ATTRACTOR

The foundation of the present work is furnished by data from a simulation of pipe flow. These simulations yielded, apparently for the first time, turbulence derived directly from the Navier–Stokes equations. The precise statement of the boundary-value problem together with its solution is given in ref. 6. It is recommended to compare the numerical methods applied there with others discussed in ref. 13. I have now a code which is

considerably faster than that of ref. 6. It permits the computation of the evolution of flow for times as long as $t = 10000$, whereas formerly $t = 500$ could only be surpassed in a few cases.

In this paper customary dimensionless units will be used throughout. These units are based on the centerline velocity of the basic flow, on the radius of the pipe, and on the kinematic viscosity of the fluid.

To ease comparison, the present analysis was made to conform as much as possible to the experimental one.[12] In particular, from the computational results the *streamwise velocity fluctuation* $u_z(t)$ was extracted as a function of time t. In cylindrical coordinates $\{\rho, \varphi, z\}$ it can be expressed as the scalar product

$$u_z(t) := \mathbf{e}_z \cdot \mathbf{u}(\rho = 0, \varphi, z = 0, t) \tag{1}$$

of the unit vector $\mathbf{e}^z$ with the disturbance $\mathbf{u}(\rho, \varphi, z, t)$. The disturbance again is nothing else than the difference between the total velocity field $\mathbf{U}$ and the basic Hagen–Poiseuille flow $\mathbf{U}^{\mathrm{HP}}$,

$$\mathbf{u}(\rho, \varphi, z, t) := \mathbf{U}(\rho, \varphi, z, t) - \mathbf{U}^{\mathrm{HP}}(\rho) \tag{2}$$

From $u_z(t)$, single-variable time series were constructed, and n_e-dimensional vectors were formed:

$$\{u_z(t), u_z(t+\tau), \ldots, u_z(t+(n_e-1)\tau)\} \tag{3}$$

As in ref. 12, these vectors were multiplied with $1/(n_e^{1/2} u_{\mathrm{rms}})$, u_{rms} being the standard deviation of the data u_z. From the vectors (3), the correlation integral $C(r)$ was evaluated following precisely Grassberger and Procaccia's prescription.[3] This was very easy indeed: The core of the code, available from the author upon request, comprises less than 20 statements.

In order to visualize salient trends, it is convenient to plot the *slope function*

$$S(r_i) := \frac{\log C(r_{i+1}) - \log C(r_{i-1})}{\log r_{i+1} - \log r_{i-1}} \tag{4}$$

The set $\{r_i \mid i = 1, \ldots, n\}$ of radii for which the correlation integral was actually computed can be seen in Figs. 1, 3, and 4.

Figure 1 displays a typical result: With decreasing radius r, the slope S approaches the embedding dimension n_e. Thus, *there is no strange attractor with dimension lower than* 20. Similar pictures were made for numerous other trajectories, with up to 10,000 vectors. In most cases the approach to the asymptotic values came out even better than in Fig. 1.

Figure 1 is nearly identical with Fig. 3 in ref. 12. This means that

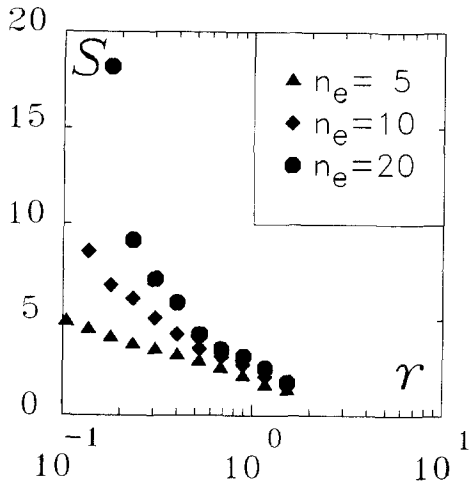

Fig. 1. Slope S as a function of the correlation radius r for various embedding dimensions n_e. The results are based on about 1500 vectors of the type (3) with $\tau = 2$. The Reynolds number of the source trajectory was $Re = 2000$. The trajectory was started at initial values as defined in ref. 6 by Eq. (36) with $a_0 = 0.2$. If there were a strange attractor with fractal dimension, say, $\nu = 1.8...$, one would expect that the slopes reach 1.8... for small radii r, but do not pass it. And this very behavior should show up in all embedding spaces with $n_e > \nu$. Figure 4 seems to be an example for such a case.

experimental and theoretical results on pipe flow almost coincide. The differences are the following: In the theoretical analysis the embedding dimension was not increased beyond 20, as this would amount to overstraining the Grassberger–Procaccia method. Second, the slopes for $n_e = 20$ are somewhat smaller in theory than in experiment. This, however, does not come as a surprise, because the experiment was done with a Reynolds number 14 times as high as in the computation.

The third item to be remarked in Fig. 1 is the excellent convergence with respect to the number of the vectors. Obviously it is possible to obtain valid information using only 1500 vectors.

Our simulation[6] has two advantages over recent experimental work[12]: First it was done for comparatively small Reynolds numbers ($Re \leqslant 3000$), where there is more hope to find a low-dimensional strange attractor than at $Re = 28{,}500$. Second, the level of undefined perturbations is in a stable computation certainly several orders of magnitude lower than even in the best experiment. This permits a clearer distinction between randomness which comes from the environment and randomness produced by the flow itself. The point is important because it is usually claimed that a picture like Fig. 1 indicates the predominance of external noise.[3] This, however, is not necessarily so, as we will see in the next section.

3. TRANSIENTS

The fun with Fig. 1 is that it is a pretender. The trajectory from which it is taken looks like turbulence for times $t < 3000$, but at $t \approx 3150$ it calms down (cf. Fig. 2).

The *average* lifetime $\bar{t}_{\text{turb}}$ of such a turbulent transient depends drastically on the Reynolds number. The word *average* was emphasized since slightly different initial conditions yield very different lifetimes. What I can guess after a few tests for some Reynolds numbers are the following order-of-magnitude estimates: $\bar{t}_{\text{turb}} \approx 500$ for $Re = 2000$, $\bar{t}_{\text{turb}} \approx 3000$ for $Re = 2500$, and $\bar{t}_{\text{turb}} > 10{,}000$ for $Re = 3000$.

This sort of transient is completely compatible with experiments. As it turns out now, the comparison of computational results with experiments as described in ref. 6 was based on transients. This, however, does not diminish the reasonable agreement reached there for the *double threshold*, for the *mean velocity*, for the *velocity fluctuations*, and for the *resistivity*. Also the good agreement of such results as shown in Fig. 1 with Sieber's findings[12] confirms that an acceptable description of reality was found.

Furthermore, eigenvalue analysis of the simulations[6] allowed one

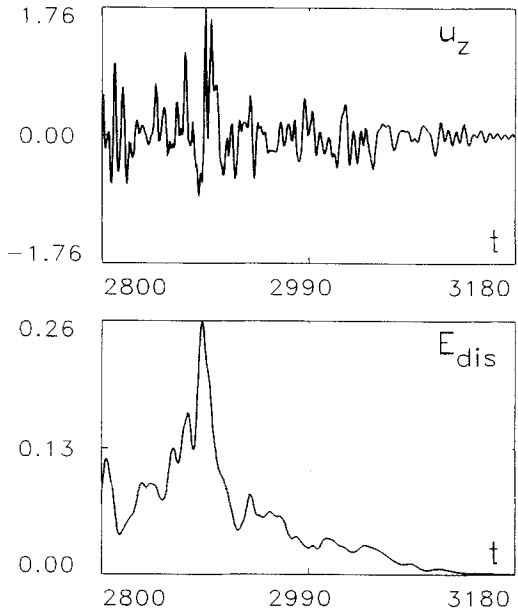

Fig. 2. Centerline velocity fluctuation u_z and energy E_{dis} as functions of time. Shown is the end of a transient. For times $0 < t < 2800$ the curves look as jagged as for $2800 < t < 3000$. The basis is the same trajectory as used for Fig. 1.

to trace the origin of pipe turbulence back to a certain property of the linearized problem, namely its *deficiency*. This deficiency divides all possible flow modes in two classes, *mothers* and *daughters*. The mothers feed the daughters by a *linear mechanism*, and the daughters make the great fuss called turbulence. Nevertheless, if it were only for linear interactions, mothers would die, and then also the daughters disappear. The *nonlinearity* reshuffles the modes and thus regenerates mothers. Essential here is the randomness of the reshuffle: The nonlinearity does not care whether it recreates mothers or daughters. But with increasing Reynolds number the mothers outmatch the daughters, so that the probability for the nonlinear regeneration of a daughter gets exceedingly small. Yet it may happen that the nonlinearity misses the mothers, and this will kill the turbulent motion. Hence, mothers and daughters do not guarantee permanence, in marked contrast to chaos, which is built on linear instabilities.

Transients with lifetimes as long as $t_{\text{turb}} = 10{,}000$ cannot reveal their true identity in an experiment, for $t_{\text{turb}} = 10{,}000$ means that a turbulent burst must migrate through a pipe which has a length of 10,000 radii before it is quenched. But for Reynolds numbers below 3000, the transients show up. And in fact, intermittency can be related to them. Intermittency in a pipe at $Re = 2500$ includes patches of laminar flow. In these patches, the level of turbulence is not only somewhat decreased as in high-Reynolds-number intermittency, it is exactly zero.[14] The initialization of a new burst requires a disturbance from outside, or, in other words, intermittency in pipe flow rests on randomness from the environment. This explains the variety in the experimental reports when quantitative results are at stake (see, for example, the discussion of "puffs" and "slugs" and the comparison with Rotta's data by Wygnanski and Champagne[15]).

The most interesting features of these transients are their lifetimes as compared with the lifetimes obtained from linear analysis. For example, for $Re = 2000$ the longest lifetime from linear analysis is $t_{\text{lin}} \approx 20$ (this is just the inverse of $-c_r$ in Fig. 23 of ref. 6. The life of the turbulent transient shown in Fig. 2 lasts 150 times longer.

4. AGING

The phase space accessible to an *autonomous dissipative system* shrinks steadily as time goes on.[2] Hence, also the transient trajectories must age continuously. But it is difficult to observe this in Fig. 2. In such plots, it always looks as if the turbulent transient stays youthful until it suffers a sudden death.

Grassberger–Procaccia analysis, however, determines directly the fill

of the phase space. Due to its fast convergence this method should be applicable for quite short pieces of a trajectory.

What is the meaning of such a picture as Fig. 1? That all the slopes reach, for sufficiently small r, the embedding dimension, signals a pretty complete spread in the phase space: The transient romps so wildly around that it does not seem to omit any subspace. But it matters also at which radius the embedding dimension is reached: When the value of r for which this happens is small, we know that there is just a small-scale rampage. But when the respective r is large, the conquest of space takes place with large random jumps. Hence we expect that the slopes (4) taken from an exhausted part of a transient should be lower than the slopes from a fresh part. This is in fact true (see Fig. 3). For large values of r, the differences cannot show up because all slopes must approach 0 for $r \to \infty$. For small values of r, the embedding dimension is reached. Therefore, again, no differences show up. But in the intermediate region one perceives the signature of aging.

An experimental investigation of intermittent pipe flow using this tool should be not too difficult. In such a study, it is of utmost importance to keep uncontrolled perturbations away from the pipe, and it is probably most rewarding to look preferentially for flows at $Re \approx 2000$.[16]

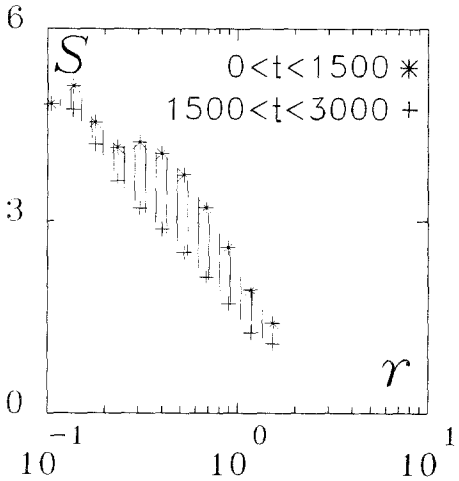

Fig. 3. Similar to Fig. 1. For this picture, the trajectory was split into two parts, as indicated in the right upper corner of the figure, and Grassberger–Procaccia analysis was performed for each part separately. The stars display the results from the fresh part, whereas crosses come from the exhausted piece. Hatching was applied to make the essential difference conspicuous. This picture was made for the embedding dimension $n_e = 5$. As with all figures in this paper, this is just one example for many others where similar trends were observed.

5. SUMMARY

The days when the strange attractor was believed to be a generally valid model of turbulence (ref. 17; see also ref. 2, Chapter 6, and ref. 18) belong to the past. The example just produced refers only to pipe flow close to the onset of turbulence. But since all shear flows are similar in their basic physics, there is little doubt that the result presented here applies to a broad class of fluid motion: Turbulence in shear flows consists of transients.

These turbulent transients are wondrous. They survive for *very* long times, but within rather short times they manage to visit considerable parts of the phase space. These peculiarities would not exist without nonlinearity.

Without perturbations from outside, turbulence in pipe flow can neither begin nor persist. But very weak and rare perturbations are sufficient. The spread of the turbulent transient in phase space is therefore an *internal* property of the transient. In other words, the *external noise* is just the trigger but not reason for the erratic flow.

Much of the work done for nonlinear dynamics was concerned with the properties of strange attractors. It might seem that all this is without meaning for the turbulent transients. Fortunately, prospects are better. The techniques developed for strange attractors are mostly methods to characterize the visits of a trajectory in the various quarters of phase space. They deliver information which is as important for transients as for trajectories on a strange attractor. In this paper, the Grassberger–Procaccia method was slightly modified to monitor the aging of turbulent transients. Aging of transients is a question of great practical importance for the controlled suppression of turbulence.

APPENDIX: DO NOT TAKE AN ARBITRARY VARIABLE

Sieber[12] pointed to some misleading effects caused by data taken with too small time differences. For example, if the single-variable time-series technique is employed, the vectors $\{x(t), x(t+\tau),..., x(t+(n_e-1)\tau)\}$ built from some variable $x(t)$ are not useful when τ is too small. Clearly, for $\tau \to 0$ we rediscover the dimension of the trajectory, viz. 1. I add here a warning of another trap.

The choice of the variable from which the time series and the vectors are constructed matters very much. For Fig. 4 the same analysis was performed as for Fig. 1, but with $x(t) = E_{\text{dis}}(t)$, where $E_{\text{dis}}(t)$ is the energy of the disturbance. The picture seems to indicate the existence of a less than two-dimensional strange attractor.

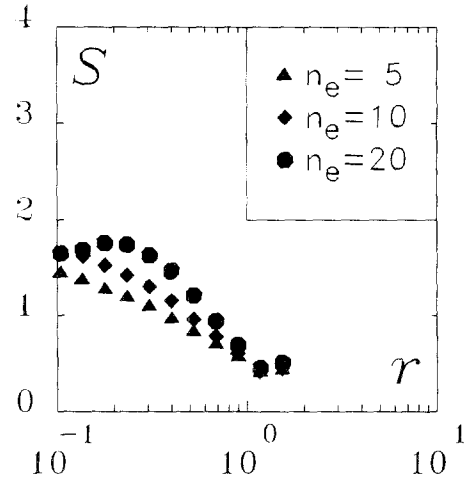

Fig. 4. Almost the same as Fig. 1. The only difference is the variable used to set up the time series: here it is the energy $E_{\text{dis}}(t)$ of the disturbance. Note the smaller scale of S.

For the disturbance defined by Eq. (2), this energy is

$$E_{\text{dis}}(t) := \tfrac{1}{2} \int_{(\text{pipe})} \mathbf{u}(\mathbf{r}, t)^2 \, dv \tag{A1}$$

The integration extends over a periodicity volume of the pipe.[6] Now it is plausible that this variable is an "almost conserved" quantity: At large Reynolds numbers the friction is small, and the coupling with the basic Hagen–Poiseuille flow occurs on a scale of around 50 time units since this is the typical lifetime of a mother–daughter pair (see Fig. 13 in ref. 6). As can be seen in Fig. 2, $E_{\text{dis}}(t)$ varies in a much slower manner than $u_z(t)$, so that the τ used for the analysis with $E_{\text{dis}}(t)$ has to be much larger than that with $u_z(t)$.

We have thus an example that even for a fixed system the check on short-time correlations has to be performed for every variable anew.

ACKNOWLEDGMENTS

Discussions with S. Grossmann saved much of my time. It was a pleasure to use the excellent facilities in the HLRZ at the KFA.

REFERENCES

1. P. Grassberger, Information content and predictablity of lumped and distributed dynamical systems, in *Proceedings of the Conference on Chaos and Related Non-linear Phenomena*, Kiryat Anavim, December 1986, preprint University of Wuppertal WU V 87–8.

2. H. G. Schuster, *Deterministic Chaos* (VCH Verlagsgesellschaft, Weinheim, 1988), Chapter 5.
3. P. Grassberger and I. Procaccia, *Physica* **9D**:189 (1983).
4. H. L. Swinney and J. P. Gollup, eds., *Hydrodynamic Instabilities and the Transition to Turbulence* (Springer, New York, 1985).
5. M. Nishioka, S. Ida, and Y. Ichikawa, *J. Fluid Mech.* **72**:731 (1975).
6. L. Boberg and U. Brosa, *Z. Naturforsch.* **43a**:697 (1988).
7. J. Guckenheimer and G. Buzyna, *Phys. Rev. Lett.* **51**:1438 (1983).
8. B. Malraison, P. Atten, P. Berge, and M. Dubois, *J. Phys. Lett.* (Paris) **44**:L-897 (1983).
9. M. Giglio, S. Musazzi, and U. Perini, *Phys. Rev. Lett.* **53**:2402 (1984).
10. A. Brandstäter, J. Swift, H. L. Swinney, A. Wolf, J. D. Framer, E. Jen, and P. J. Crutchfield, *Phys. Rev. Lett.* **51**:1442 (1983).
11. A. Brandstäter, H. L. Swinney, and G. T. Chapman, in *Dimensions and Entropies in Chaotic Systems*, G. Mayer-Kress, ed. (Springer, Berlin, 1986), p. 150.
12. M. Sieber, *Phys. Lett. A* **122**:467 (1987).
13. C. Canuto, M. Y. Hussaini, A. Quarteroni, and T. A. Zang, *Spectral Methods in Fluid Mechanics* (Springer, New York, 1988).
14. O. Reynolds, *Phil. Trans.* **174**:935 (1883).
15. I. J. Wygnanski and F. H. Champagne, *J. Fluid Mech.* **59**:281 (1973).
16. J. Meseth, *Arch. Mech.* **26**:391 (1974).
17. F. Takens, in *Dynamical Systems and Turbulence*, D. A. Rand and L. S. Young, eds. (Springer, Berlin, 1981), p. 366.
18. O. E. Lanford, in *Hydrodynamic Instabilities and the Transition to Turbulence*, H. L. Swinney and J. P. Gollup, eds. (Springer, New York, 1985).

Communicated by D. Stauffer